Computer Modeling Studies of Ribonuclease T_1–Guanosine Monophosphate Complexes

P. V. BALAJI,[1] W. SAENGER,[2] and V. S. R. RAO[1]

[1]Molecular Biophysics Unit, Indian Institute of Science, Bangalore 560 012, India, and [2]Institute for Crystallography, Free University Berlin, Takustrasse 6, D-1000 Berlin 33, Federal Republic of Germany

SYNOPSIS

The three-dimensional structures of ribonuclease (RNase) T_1 complexes with the inhibitors 2′-guanylic acid (2′-GMP), 3′-guanylic acid (3′-GMP), and 5′-guanylic acid (5′-GMP) were predicted by energy minimization studies. It is shown that these inhibitors can bind to RNase T_1 in either of the ribose puckered conformations (C2′-*endo* and C3′-*endo*) in solid state and exist in significant amounts in both forms in solution. These studies are in agreement with the x-ray crystallographic studies of the 2′-GMP–Lys25–RNase T_1 complex, where the inhibitor binds in C2′-*endo* puckered conformation. These results are also in good agreement with the available ^{1}H-nmr results of Inagaki et al. [(1985) *Biochemistry* **24,** 1013–1020], but differ from their conclusions where the authors favor only the C3′-*endo* ribose conformation for all the three inhibitors. The calculations explain the apparent discrepancies in the conclusions drawn by x-ray crystallographic and spectroscopic studies. An extensive hydrogen-bonding scheme was predicted in all the three complexes. The hydrogen-bonding scheme predicted for the 2′-GMP (C2′-*endo*)–RNase T_1 complex agrees well with those reported from x-ray crystallographic studies. In all three complexes the base and the phosphate bind in nearly identical sites independent of the position of the phosphate or the ribose pucker. The glycosyl torsion angle favors a value in the +*syn* range in the 2′-GMP(C2′-*endo*)–RNase T_1, 3′-GMP(C2′-*endo*)–RNase T_1, and 3′-GMP(C3′-*endo*)–RNase T_1 complexes; in the high-*syn* range in the 2′-GMP(C3′-*endo*)–RNase T_1 complex; and in the -*syn* range in the 5′-GMP(C2′-*endo*)–RNase T_1 and 5′-GMP(C3′-*endo*)–RNase T_1 complexes. These results are in agreement with experimental studies showing that the inhibitory power decreases in the order 2′-GMP > 3′-GMP > 5′-GMP, and they also explain the high pK_a value observed for Glu58 in the 2′-GMP–RNase T_1 complex.

INTRODUCTION

Ribonuclease T_1 (RNase T_1; EC 3.1.27.3) catalyzes the endonucleolytic hydrolysis of the phosphodiester linkage on the 3′ side of the guanine bases in single-stranded RNA with very high specificity and serves as an invaluable tool in the structural analysis of nucleic acids. A variety of physicochemical techniques like CD, uv, nmr, kinetic, and chemical modification studies have been applied to elucidate the specific recognition of guanine by RNase T_1. From kinetic studies[1,2] on guanine mononucleotides it has been shown that the inhibitory effect decreases in the order 2′-guanylic acid (2′-GMP) > 3′-guanylic acid (3′-GMP) > 5′-guanylic acid (5′-GMP). The pK_a of Glu58 has been determined to be between 4.1 and 4.9 in the free protein[3–6] and 7.8 in presence of 2′-GMP.[3] The mononucleotide inhibitors were shown to bind to the enzyme in the monoionic form with a single negative charge.[5,7,8] However, the information obtained from these studies[9,10] is not sufficient to unequivocally establish either the probable binding orientations of these inhibitors or the nature of interactions responsible for the specific recognition of the guanine base. The exact role played by different amino acid residues shown to be involved

CCC 0006-3525/90/3-40257-16 $04.00
Biopolymers, Vol. 30, 257–272 (1990)

in binding and/or catalysis by chemical modification studies is also not clear.

Recent x-ray crystallographic studies on the 2′-GMP–RNase T_1 complex at 1.9 Å resolution[11] showed that the ribose moiety of the bound 2′-GMP molecule adopts a C2′-*endo* puckered conformation. The mode of binding of 2′-GMP to native RNase T_1 determined crystallographically at a resolution of 1.9 Å[12] is in fairly good agreement with the one found in the 2′-GMP–Lys25–RNase T_1 complex. Although both these studies agree with each other regarding the puckering of the ribose and the conformation of the bound 2′-GMP molecule around the glycosyl bond [+synclinal (+*syn*) range], they differ in the nature of the hydrogen bonds between 2′-GMP and the protein (Table I). From ^{1}H-nmr investigations on the complexes of RNase T_1 with the four inhibitors 2′-GMP, 3′-GMP, 5′-GMP, and guanosine 3′,5′-bis(phosphate) it was suggested that 2′-GMP and 3′-GMP adopt the C3′-*endo syn* conformation and 5′-GMP and guanosine 3′,5′-bis(phosphate) adopt the C3′-*endo anti* conformation when bound to RNase T_1.[13] Thus the puckering of the ribose moiety in the 2′-GMP–RNase T_1 complex seems to be different in solution from that observed in the solid state.

A low-resolution (2.6 Å) crystal structure determination of RNase T_1 with 3′-GMP,[14] an inhibitor and the product of the catalyzed reaction, could not provide much information about the ribose pucker or about the hydrogen bonds between the phosphate and the protein reportedly because of static disorder in the crystal. The crystal structure of the enzyme complexed with 5′-GMP has not been determined so far. There is therefore no data that can show whether in the solid state 3′-GMP and 5′-GMP also adopt conformations that are different from the ones proposed from solution studies. In view of this a computer modeling study has been taken up to investigate the favored modes of binding of the three mononucleotide inhibitors 2′-GMP, 3′-GMP, and 5′-GMP to RNase T_1. These studies not only provide information regarding the probable modes of binding and the possible hydrogen bonds between these inhibitors and the protein, but also provide a stereochemical explanation for the observed experimental results, particularly the differences observed in the puckering of the ribose moiety of 2′-GMP in solid state and solution. Further, being a small protein of 104 amino acid residues, RNase T_1 serves as a good model system to understand how proteins recognize base sequences in single-stranded RNA molecules.

Table I Proposed Hydrogen-Bonding Scheme for the 2′-GMP–RNase T_1 Complex

	X-Ray Diffraction Study		Present Calculation
	Native[a] RNase T_1	Lys25–[b] RNase T_1	C2′-*endo* Complex
N1	E46 OE1	E46 OE1	E46 OE1
N2	N98 O	N98 O	N98 O
		E46 OE2	E46 OE2
O6	N44 N	N44 N	N44 N
		Y45 N	Y45 N
N7	N43 ND2		N43 ND2
	N43 N	N43 N	N43 N
O2′			H40 NE2
			E58 OE2
O5′			N98 OD1
OP1		Y38 OH	H92 NE2
		H40 NE2	
OP3	Y38 OH	E58 OE2	Y38 OH
	E58 OE2		E58 OE1
	R77 NH2		R77 NE

[a] Sugio et al.[12]
[b] Arni et al.[11]

METHODS

All the calculations reported in this paper use the protein coordinates from a 2′-GMP–Lys25–RNase T_1 complex solved at a resolution of 1.9 Å.[11] The coordinates for the various inhibitors (Figure 1a–c) were generated using standard geometry.[15–17] The conventions followed for defining the torsion angles in the nucleotide unit were the same as described by Saenger.[16] The polar hydrogen atoms were fixed using standard bond lengths and bond angles.[18] Some approximations were made in the present study to simplify the calculations and to reduce the required computation time. Although the 2.6 Å resolution x-ray crystal structure study of the 3′-GMP–RNase T_1 complex[14] could not provide much information about the ribose pucker and the hydrogen bonds between the phosphate group and RNase T_1, the overall polypeptide folding was found to be similar to that observed in the 2′-GMP–RNase T_1 complex. In view of this it was assumed that the backbone conformation would be the same in the complex of 5′-GMP with RNase T_1 also, and hence in all cases only the side-chain atoms of the amino acids were allowed to move during minimization. All CH, CH_2, and CH_3 groups in the protein and the inhibitor molecule were treated as united atoms while computing the total conformational energy. In the 1.9

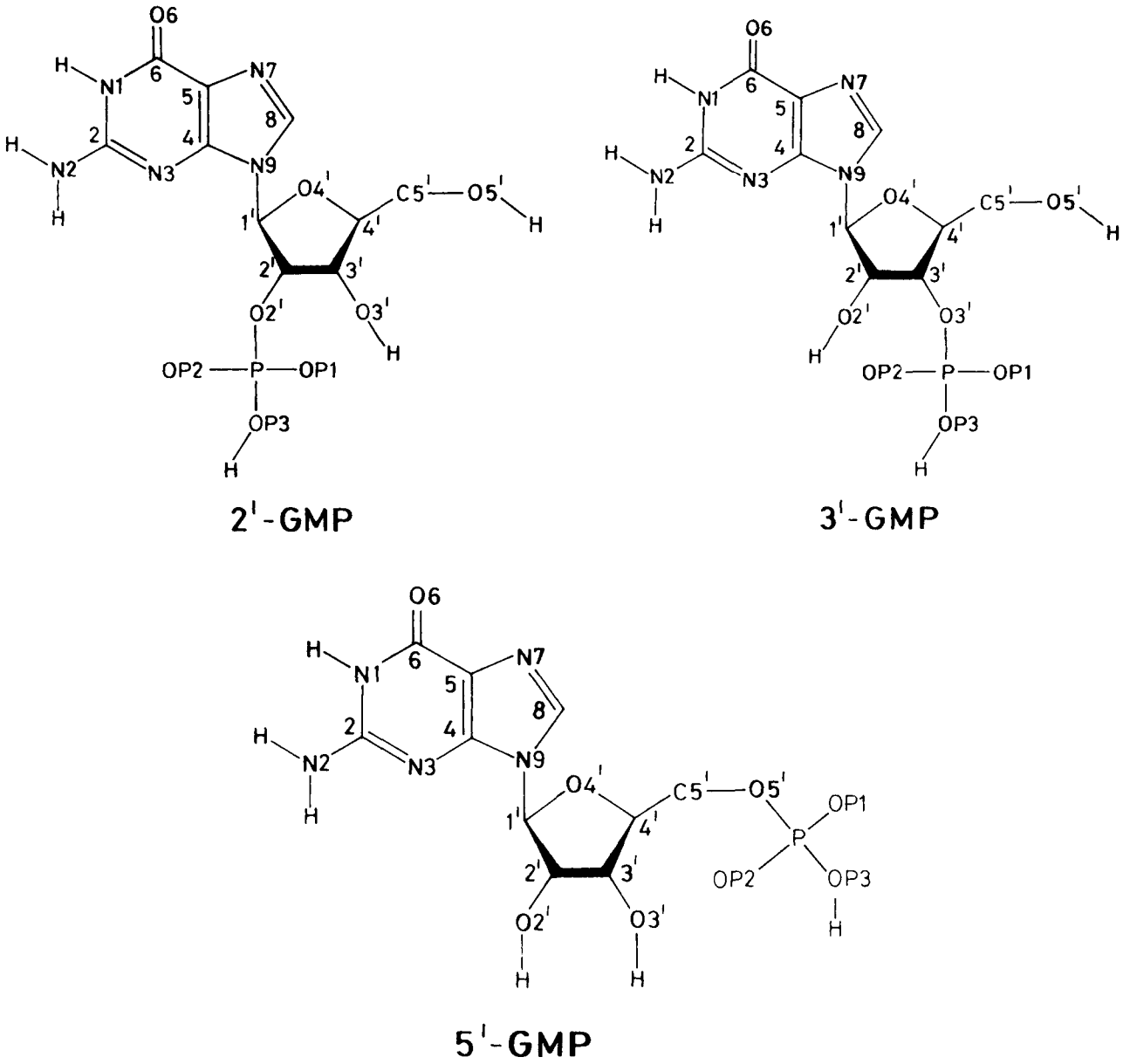

Figure 1 Cartoon diagrams of the three inhibitors 2′-GMP, 3′-GMP, and 5′-GMP studied in the present work along with the nomenclature used.

Å resolution crystal structure study of the 2′-GMP–Lys25–RNase T_1 complex,[11] most of the water molecules were found around the surface of the protein and sparsely in the active site, and the inhibitor binding site was found to be part of an apparently underhydrated surface portion. Hence instead of including the solvent molecules explicitly, the effect of solvent in damping the electrostatic forces was modeled by using a distance-dependent dielectric constant which weighs the short-range interactions more than the long-range interactions.

First, the sterically allowed orientations for the inhibitor in the active site were identified using "contact criteria." Initially, the guanine base was fixed in the binding site of the protein as identified in the solid state.[11] For this the center of the six-membered ring of the guanine base was taken as the origin of the right-handed Cartesian coordinate system. The three rotational parameters specified in terms of the three Eulerian rigid body rotation angles—ϕ, θ, and ψ—define the orientation of the base in the binding site. All the amino acid residues that

fall within a sphere of radius 10 Å from the center of the base were considered for contact criteria. For determining the sterically allowed orientations for the base only, the backbone atoms were considered. The base was rotated by varying each one of the three rotation angles in steps of 10° (ϕ from 0° to 360°, θ from 0° to 180°, and ψ from 0° to 360°) and then translated into the binding site. An orientation was rejected as disallowed if the distance between any inhibitor atom and any protein atom was less than the contact criterion specified for that particular atom pair.[19] The ribose moiety was then attached to guanine at different glycosyl torsion angles (10°, 90°, 180°, and 270°) and in both C2′-*endo* and C3′-*endo* puckered conformations to find out the allowed orientations for guanosine in the binding site starting from only those orientations allowed for guanine.

Subsequently, the sterically allowed orientations for the guanosine were used as starting points for energy minimization of the 2′-GMP, 3′-GMP, and 5′-GMP (both C2′-*endo* and C3′-*endo* puckering modes) complexes with RNase T_1. About 15–20 orientations in the sterically allowed region were selected as starting points for minimization of the complexes of each of the three inhibitors with RNase T_1 covering the entire allowed region. Minimization was also carried out with different conformations of the amino acid side chains (other than those observed in the crystal structure) and the inhibitor as starting conformations. All the 104 amino acid residues in the protein were considered for calculating the energy. Since the coordinates for the side-chain atoms of Glu102 were not available from the x-ray study due to orientational disorder, they were fixed using the standard geometry in staggered orientations.[20] All the acidic and basic amino acid residues and the terminal amino and carboxyl groups were considered as ionized except Glu58, which was treated as neutral.[3] The phosphate group of the inhibitor was considered in its monoionic form carrying one negative charge.[5,7,8] The side-chain atoms of 37 amino acid residues including those involved in guanine recognition and in catalysis, i.e., Ser35 to Phe50, Tyr56 to Ile61, Tyr68 to Val79 and Val89 to Glu102 (Table II) were allowed to move during energy minimization. The total calculated energy includes the intramolecular energy of the inhibitor and the protein and the interaction energy of the inhibitor with the protein. This was calculated by considering the van der Waals, electrostatic, hydrogen-bond, and torsional contributions. The van der Waals energy was evaluated using the Lennard-Jones 6–12 potential and the electrostatic energy using the Coulomb expression. The hydrogen-bond contribution was evaluated using the 10–12 potential instead of the van der Waals 6–12 potential only for those atom pairs that had the potential to form a hydrogen bond (i.e., between polar hydrogen atoms and atoms of the type $-N=$, $-O-$, and $=O$ that can act as hydrogen-bond acceptors). The function used was of the form

$$E_{\text{tot}} = \frac{FA}{r^{12}} - \frac{C}{r^6} + \frac{332.0Q_iQ_j}{dr} + \frac{V}{2}[1 \pm \cos(nt)] + \frac{A'}{r^{12}} - \frac{B}{r^{10}}$$

The values of the constants A, A', B, and C were taken from Nemethy et al.[21,22] For the phosphorous atom, the parameters for the 6–12 potential were taken from Refs. 23–25. The r is the distance between the interacting atom pair. V is the height of the n-fold barrier and t is the torsion angle. The values for the parameters V and n were taken from Ref. 20 for amino acids. In the nucleotides, the torsional contribution from rotation about the glycosyl bond was taken to be zero as the barrier is presumed to be very low.[26] For other bonds the parameters were taken from Ref. 25. F is the scaling factor taken as 0.5 for 1–4 interactions (i.e., interactions between atoms separated by three bonds) and as 1.0 for 1–5 and higher interactions (i.e., interactions between atoms separated by four or more bonds). The partial charges Q_i and Q_j on the inhibitor and the protein

Table II Amino Acid Residues Whose Side Chains Were Treated as Flexible During Minimization[a]

Ser35	Asn36	Ser37	Tyr38	His40	Lys41	Tyr42	Asn43	Asn44
Tyr45	Glu46	Phe48	Asp49	Phe50	Tyr56	Tyr57	Glu58	Trp59
Ile61	Tyr68	Ser69	Ser72	Asp76	Arg77	Val78	Val79	Val89
Ile90	Thr91	His92	Thr93	Ser96	Asn98	Asn99	Phe100	
Val101	Glu102							

[a] Ala1-Gly34, Pro39, Gly47, Ser51-Pro55, Pro60, Leu62-Val67, Gly70-Gly71, Pro73, Gly74, Ala75, Phe80-Gly88, Gly94, Ala95, Gly97, and Cys103-Thr104 were kept rigid.

atoms were calculated by the CNDO/2 method.[27] For calculating the charges on the atoms of amino acid residues, the N-acetyl-N′-methyl amino acid amides were considered. For the nucleotides the charges were calculated for the guanine base and the ribose–phosphate moiety separately. In all the cases the charges were calculated for different conformations and average values were taken (Tables III and IV). The effective dielectric constant (d) was set equal to the distance between the interacting atom pair. Such a distance-dependent dielectric constant is computationally efficient as only even powers of r are then needed for energy evaluation. The total potential energy of the complex was minimized with respect to both external (3 translational and 3 rotational) and internal (7 inhibitor and 86 protein side-chain torsion angles) degrees of freedom using the double dogleg strategy of Dennis and Mei.[28] Gradients were calculated by analytical differentiation of the energy function[29] and all the calculations were done in double precision arithmetic. The minimization method employs a model trust region to choose the step length, double dogleg strategy to choose the search direction and BFGS formula to

Table III Partial Atomic Charges for Amino Acids[a]

Amino Acid	N	NH	CA	CB	C′	O	Side-Chain Atoms							
Ala	−.2017	.1229	.0734	.0231	.3452	−.3629								
Ala^{+b}	−.0020	.2500	.1200	.1320	.3500	−.3500								
Arg$^+$	−.2023	.1271	.0778	0.440	.3532	−.3594	CG	.0582	CD	.1389	NE	−.1731	HE	.1702
							CZ	.4672	NH	−.2271	HH	.1881		
Asn	−.2141	.1254	.0670	.0035	.3575	−.3626	CG	.3648	ND1	−.3027	HD1	.1541	OD2	−.3470
Asp	−.2049	.1212	.0898	.0160	.3535	−.3544	CG	.3959	OD1	−.3442	OD2	−.2468	HD2	.1739
Asp$^-$	−.2161	.1083	.0725	−.1412	.3482	−.3867	CG	.3650	OD	−.5750				
Cys	−.2024	.1296	.0890	.0395	.3560	−.3430	SG	−.0687						
Gln	−.2116	.1229	.0691	.0298	.3491	−.3603	CG	−.0069	CD	.3638	NE1	−.2591	HE1	.1291
							OE2	−.3550						
Glu	−.2105	.1214	.0729	.0354	.3567	−.3631	CG	−.0078	CD	.4017	OE1	−.3364	OE2	−.2448
							HE2	.1745						
Glu$^-$	−.2084	.1161	.1123	−.0545	.3506	−.3682	CG	−.1501	CD	.3522	OE	−.5750		
Gly	−.1924	.1231	.0711		.3546	−.3564								
His	−.2120	.1233	.0697	.0098	.3516	−.3602	CG	.0149	ND1	−.0604	HD1	.1065	CD2	.0400
							CE1	.1213	NE2	−.2045				
His$^+$	−.2026	.1246	.0944	.0764	.3335	−.3314	CG	.0920	ND1	−.0194	HD1	.1938	CD2	.1513
							CE1	.2976	NE2	−.0070	HE2	.1918		
Ile	−.2101	.1162	.0743	.0331	.3490	−.3592	CG1	.0061	CG2	−.0068	CD1	−.0026		
Leu	−.2028	.1223	.0679	.0140	.3462	−.3517	CG	.0365	CD	−.0162				
Lys$^+$	−.1996	.1255	.0739	.0467	.3460	−.3569	CG	.0542	CD	.0482	CE	.1982	NZ	−.0175
							HZ	.2271						
Met	−.2015	.1228	.0670	.0419	.3560	−.3632	CG	.0279	SD	−.0969	CE	.0460		
Phe	−.2033	.1239	.0740	.0067	.3512	−.3598	CG	.0369	CD	−.0234	CE	.0085	CZ	.0002
Pro	−.1760		.0750	.0290	.3500	−.3650	CG	.0080	CD	.0790				
Ser	−.2024	.1187	.0678	.1202	.3587	−.3614	OG	−.2421	HG	.1405				
Thr	−.2102	.1214	.0657	.1405	.3577	−.3605	OG1	−.2556	HG1	.1303	CG2	.0107		
Thr^{-c}	−.1956	.0780	.0135	.1271	.3691	−.5750	OG1	−.2760	HG1	.0872	CG2	−.0533		
Trp	−.2101	.1241	.0701	.0112	.3523	−.3609	CG	−.0537	CD1	.0751	CD2	−.0019	NE1	−.1418
							HE1	.1105	CE2	.1019	CE3	−.0107	CZ2	−.0397
							CZ3	−.0271	CH	.0007				
Tyr	−.2151	.1240	.0740	.0091	.3502	−.3601	CG	.0173	CD	.0072	CE	−.0422	CZ	.1867
							OH	−.2503	HH	.1342				
Val	−.2134	.1244	.0655	.0326	.3535	−.3648	CG	.0011						

[a] Charges are given in electronic charge units (ecu). Charges on the nonpolar hydrogen atoms have been added to the nonhydrogen atom to which they are attached.

[b] Ala$^+$ is the N-terminal alanine residue.

[c] Thr$^-$ is the C-terminal threonine residue.

Table IV Partial Atomic Charges for Nucleotides[a]

Guanine		Ribose			
Atom	Charge	Atom	Charge 2′-GMP	Charge 3′-GMP	Charge 5′-GMP
N1	−.2139	C1′	.213	.1848	.1954
C2	.3815	C2′	.1389	.0858	.0874
N3	−.3272	C3′	.1195	.1246	.1423
C4	.2117	C4′	.1379	.1686	.1238
C5	−.102	O4′	−.2672	−.2658	−.2379
C6	.3529	O2′	−.3014	−.2398	−.255
O6	−.389	H2′		.107	.1182
H1	.1205	O3′	−.2365	−.3036	−.255
N2	−.2474	H3′	.1056		.1182
H2	.1357	C5′	.1039	.1521	.1056
N7	−.1652	O5′	−.2601	−.2601	−.2811
C8	.1214	H5′	.1084	.1084	
N9	−.1202	P	.373	.373	.373
		OP1	−.4749	−.4749	−.4749
		OP2	−.4749	−.4749	−.4749
		OP3	−.3356	−.3356	−.3356
		H	.1559	.1559	.1559

[a] Charges are given in electronic charge units (ecu). Charges on the nonpolar hydrogen atoms have been added to the non-hydrogen atom to which they are attached.

update the Hessian and the inverse Hessian approximations. Minimization was stopped when the rms gradient was less than 0.01 kcal/mol/Å. This minimization method was implemented and coded in the authors' laboratory to study the T4-lysozyme–ligand interactions.[30] Scheraga and co-workers have used a similar algorithm implemented by Gay[31] to study the interactions between two β sheets in a protein,[32] to study the multiple minimum problem in protein folding by Monte Carlo minimization approach,[33] and to predict the conformations for the immunodominant region of the circumsporozoite protein of the human malaria parasite *Plasmodium falaparum*.[34]

RESULTS

From contact criteria, it was found that the guanine base can bind in mainly two modes. In one mode, the orientation of the base was similar to that observed in the crystal structure and in the other, it binds in a "flipped" orientation. When energy minimization was carried out starting from the sterically allowed orientations identified by contact criteria, in all the minimized conformers, the base assumed either of these two orientations. However, the total energy was very high in those complexes in which the base binds in a flipped orientation. Tables V–VII show some of the low-energy conformers of the complexes of the three inhibitors with RNase T_1. In all the low-energy conformers of a particular complex the base hydrogen bonds remained the same [except in the 3′-GMP(C3′-*endo*)– and the 5′-GMP(C3′-*endo*)–RNase T_1 complexes], and the phosphate was bound in the pocket formed by residues Asn36, Tyr38, His40, Glu58, Arg77, His92, and Asn98. The energy difference between the lowest and other conformers was mainly from the movement of the amino acid residues present in the phosphate binding pocket.

Only the lowest energy conformers of the complexes of the three mononucleotide inhibitors 2′-GMP, 3′-GMP, and 5′-GMP in both C2′-*endo* and C3′-*endo* puckered conformations with RNase T_1 are reported in Table VIII (Figure 2a–f). In Table IX, the possible hydrogen bonds between the inhibitor and the protein predicted from the present calculations are shown. The orientations of the side chains of many of the amino acid residues are significantly altered from those reported from the crystal structure, and these are shown in Table X.

The base binding site comprises mainly the residues Tyr42, Asn43, Asn44, Tyr45, Glu46, Asn98, and Phe100 in all the three RNase T_1–inhibitor complexes (Figure 2a–f). N1 of guanine is hydrogen bonded to Glu46 OE1 in all the cases. N2 of the base forms two hydrogen bonds: one with Glu46 OE2 and the second with the backbone oxygen of Asn98. The latter hydrogen bond is not possible in the 3′-GMP(C3′-*endo*)–RNase T_1 complex. O6 of the base accepts two hydrogen bonds from Asn44 N and Tyr45 N. Both these hydrogen bonds with O6 are not possible in the 5′-GMP(C3′-*endo*)–RNase T_1 complex. N7 forms a hydrogen bond with both Asn43 N and Asn43 ND2 in the complexes of 2′-GMP and 3′-GMP with RNase T_1, and only with Asn43 ND2 in the complexes of 5′-GMP with RNase T_1.

The ribose moiety of all the three inhibitors in both C2′-*endo* and C3′-*endo* puckered conformations forms a hydrogen bond with the Asn98 side-chain amide group, but this is rather weak in the 5′-GMP–RNase T_1 (both C2′-*endo* and C3′-*endo*) complexes (Figure 2e and f; Table IX). In addition to this hydrogen bond, O2′ forms two hydrogen bonds in the 2′-GMP(C2′-*endo*)–RNase T_1 complex (with His40 NE2 and Glu58 OE2; Figure 2a) and the 3′-GMP(C2′-*endo*)–RNase T_1 complex (with Glu58 OE1 and OE2; Figure 2c). In the 3′-GMP(C3′-

Table V Low-Energy Conformers of the 2′-GMP–RNase T_1 Complex[a]

	C2′-*endo*			C3′-*endo*			
No.	1	2	3	1	2	3	4
X	14.9	14.9	14.9	15.	14.9	15.1	14.9
Y	33.4	33.4	33.4	33.4	33.5	33.4	33.5
Z	21.2	21.2	21.4	21.	21.1	21.	21.2
ϕ	190.2	189.8	190.5	214.7	206.6	197.7	200.1
θ	150.4	149.	150.4	152.1	150.2	150.7	149.9
ψ	33.	31.2	31.5	53.5	45.3	41.9	36.9
χ	85.3	81.9	82.	137.	133.7	117.5	115.
O2′	H40 NE2 E58 OE2	E58 OE2	E58 OE2				
O3′				N98 OD1	N98 OD1	N98 OD1	N98 OD1
O5′	N98 OD1						
OP1	H92 NE2	H92 NE2	Y38 OH R77 NE	R77 NH2 H92 NE2	Y38 OH	N36 ND2	E58 OE2
OP2			H92 NE2	Y38 OH E58 OE2	E58 OE2	Y38 OH E58 OE2	Y38 OH
OP3	Y38 OH R77 NE	Y38 OH R77 NE	N36 ND2		R77 NH2 H92 NE2	H92 NE2	H92 NE2
H	E58 OE1	E58 OE1	Y38 OH	E58 OE1		N98 OD1	
ENE	0.	4.4	6.7	0.	3.	4.	6.

[a] The base hydrogen bonds in all the conformers are same and are shown in Table IX for the lowest energy conformers. Rigid body rotation angles ϕ, θ, and ψ and the glycosyl torsion angle χ are in degrees. Energy is relative to Conformer No. 1.

Table VI Low-Energy Conformers of the 3′-GMP–RNase T_1 Complex[a]

	C2′-*endo*			C3′-*endo*		
No.	1	2	3	1	2[b]	3[b]
X	14.8	14.8	14.8	14.9	14.9	14.9
Y	33.5	33.6	33.5	33.1	33.2	33.1
Z	21.3	21.2	21.2	21.6	21.6	21.4
ϕ	211.8	212.6	108.9	183.4	182.	173.9
θ	145.	147.8	147.1	138.9	139.	154.4
ψ	43.4	45.4	42.4	22.8	23.	17.3
χ	87.7	100.4	97.5	6.8	6.3	16.7
O2′	E58 OE1 E58 OE2	E58 OE2	E58 OE2			
O3′					N36 ND2	N36 ND2
O5′	N98 OD1			H92 NE2 N98 OD1	N98 OD1	H92 NE2
OP1	N36 ND2 Y38 OH	N36 ND2 Y38 OH	N36 ND2 Y38 OH	Y38 OH H40 NE2 R77 NE R77 NH2	Y38 OH H40 NE2 R77 NH2	
OP2	R77 NH2 H92 NE2	R77 NH2 H92 NE2	R77 NH2 H92 NE2			N36 ND2 Y38 OH R77 NH2
OP3					H92 NE2	H40 NE2
H				E58 OE1	E58 OE1	
ENE	0.	.9	1.5	0.	1.3	7.4

[a] Rigid body rotation angles ϕ, θ, and ψ and glycosyl torsion angle χ are in degrees. Energy is relative to Conformer No. 1. The base hydrogen bonds are same as given in Table IX for the low-energy conformers. [b]An additional N2–N98 O hydrogen bond is formed.

Table VII Low-Energy Conformers of the 5′-GMP–RNase T_1 Complex[a]

	C2′-*endo*			C3′-*endo*		
No.	1	2	3	1	2[b]	3[c]
X	15.	14.9	14.9	15.3	14.9	15.2
Y	33.5	33.4	33.4	33.5	33.4	33.5
Z	21.6	21.7	21.8	21.7	21.9	21.8
ϕ	169.8	162.5	148.4	160.4	141.9	153.6
θ	150.8	154.	154.1	149.3	156.2	148.8
ψ	7.8	0.5	−10.6	−7.8	−18.8	−10.8
χ	307.1	297.4	319.8	286.8	299.6	288.1
O4′	N98 ND2			N98 ND2		
O5′		H40 NE2	N98 ND2			
		E58 OE2				
OP1	H92 NE2	Y38 OH	R77 NE	H92 NE2	R77 NE	R77 NH2
	N98 ND2	R77 NE	R77 NH2	N98 ND2	R77 NH2	H92 NE2
		R77 NH2	H92 NE2		R77 NE	
OP2	R77 NH2	H92 NE2	Y38 OH	R77 NH2	Y38 OH	Y38 OH
	H92 NE2	N98 ND2	H40 NE2	H92 NE2	H40 NE2	E58 OE2
OP3	Y38 OH		E58 OE2	Y38 OH	E58 OE2	N98 ND2
	R77 NE			E58 OE2		
H	E58 OE1		E58 OE1	E58 OE1	E58 OE1	
ENE	0.	1.2	5.9	0.	3.6	5.6

[a] Rigid body rotation angles ϕ, θ, and ψ and glycosyl torsion angle χ are in degrees. Energy is relative to Conformer No. 1. The base hydrogen bonds are same in all conformers as given in Table IX for the minimum energy conformer, and in addition, the 06–N44 N hydrogen bond in (b) and (c) and 06–Y45 N hydrogen bond in (b) are formed.

endo)–RNase T_1 complex (Figure 2d), the O5′ atom forms a hydrogen bond with His92 NE2.

Although the position of the phosphate group is different in the three inhibitors, present calculations predict that the phosphate group always prefers to bind in the same site of the protein comprising the residues Asn36, Tyr38, His40, Glu58, Arg77, His92, and Asn98 (Figure 2a–f; Table IX). The phosphate group donates a hydrogen atom to Glu58 in all the three RNase T_1–inhibitor complexes except in the 3′-GMP(C2′-*endo*)–RNase T_1 complex, where the 2′-OH group acts as the donor. Asn36 ND2 forms a hydrogen bond with the phosphate only in the 3′-GMP(C2′-*endo*)–RNase T_1 complex. Tyr38 OH forms one hydrogen bond with the phosphate group in all the three RNase T_1–inhibitor complexes. Although the His40 side chain is near the phosphate group in all the complexes, hydrogen-bond formation between them is possible only in the 3′-GMP(C3′-*endo*)–RNase T_1 complex. Arg77 and His92 side

Table VIII Theoretically Predicted Binding Orientations and Conformations of the Three Inhibitors in Complexes with RNase T_1

Inhibitor	Ribose Pucker	*X*, *Y*, *Z*[a]	ϕ, θ, ψ[b]	χ[c]	Energy[d]	H8-H1′ Distance
2′-GMP	C2′-*endo*	14.902, 33.397, 21.176	190.2, 150.4, 33.0	85.31	0.315	2.616
	C3′-*endo*	14.967, 33.442, 21.008	214.7, 152.1, 53.5	136.98	0.000	3.132
3′-GMP	C2′-*endo*	14.844, 33.531, 21.275	211.8, 145.0, 43.4	87.65	7.676	2.632
	C3′-*endo*	14.846, 33.107, 21.602	183.4, 138.9, 22.8	6.76	7.712	2.860
5′-GMP	C2′-*endo*	14.996, 33.463, 21.549	169.8, 150.8, 7.8	307.10	13.113	3.534
	C3′-*endo*	15.319, 33.521, 21.660	160.4, 149.3, −7.8	286.84	14.657	3.711

[a] Translational parameters.
[b] Rotational parameters (in degrees).
[c] Glycosyl torsion angle (in degrees).
[d] Total energy relative to the 2′-GMP (C3′-*endo*) complex that is the lowest.

Table IX Proposed Hydrogen-Bonding Scheme in the Complexes of the Three Inhibitors with RNase T_1 in the Minimum Energy Conformations[a,b]

	C2′-*endo*			C3′-*endo*		
	2′-GMP	3′-GMP	5′-GMP	2′-GMP	3′-GMP	5′-GMP
Guanine						
N1	E46 OE1	E46 OE1	E46 OE1	E46 OE1	E46 OE1	E46 OE1
	1.98 156.7	2.10 131.0	1.91 169.7	2.14 147.8	2.09 141.9	2.2 169.9
N2	E46 OE2	E46 OE2	E46 OE2	E46 OE2	E46 OE2	E46 OE2
	1.94 171.5	1.81 164.5	1.83 165.4	1.92 169.4	1.95 157.5	1.84 154.1
	N98 O	N98 O	N98 O	N98 O		N98 O
	1.95 149.7	2.02 172.8	1.89 160.9	2.07 141.1		1.89 160.6
O6	N44 N	N44 N	N44 N	N44 N	N44 N	
	2.21 106.5	2.44 102.6	2.31 112.5	2.45 102.4	2.13 105.6	
	Y45 N	Y45 N	Y45 N	Y45 N	Y45 N	
	1.88 164.0	1.90 173.6	2.17 167.2	1.85 175.1	1.90 164.5	
N7	N43 N	N43 N		N43 N	N43 N	
	2.11 173.1	2.46 169.6		2.18 176.0	2.23 174.2	
	N43 ND2	N43 ND2	N43 ND2	N43 ND2	N43 ND2	N43 ND2
	2.38 136.9	2.43 145.9	2.21 162.3	2.23 144.3	2.30 150.7	2.36 144.9
Ribose						
O2′	H40 NE2	E58 OE1				
	2.49 149.3	1.72 137.2				
	E58 OE2	E58 OE2				
	1.92 135.8	2.42 135.0				
O3′				N98 OD1		
				1.68 159.8		
O4′			N98 ND2			N98 ND2
			2.46 123.5			2.28 122.6
O5′	N98 OD1	N98 ND2			H92 NE2	
	1.68 161.9	2.05 116.1			1.65 153.2	
					N98 OD1	
					1.69 148.7	
Phosphate						
OP1	H92 NE2	N36 ND2	H92 NE2	R77 NH2	Y38 OH	H92 NE2
	1.84 126.8	1.82 131.6	2.22 120.6	1.86 172.9	1.67 143.7	2.05 126.5
		Y38 OH	N98 ND2	H92 NE2	R77 NE	N98 ND2
		1.65 142.0	2.33 148.1	1.81 157.7	2.47 124.2	1.87 146.2
					R77 NH2	
					1.91 139.9	
OP2		R77 NH2	R77 NH2	Y38 OH	H40 NE2	R77 NH2
		1.91 162.0	1.85 174.4	1.66 174.6	1.85 123.3	1.81 162.4
		H92 NE2	H92 NE2	E58 OE2		H92 NE2
		1.81 142.3	2.06 121.5	1.70 152.8		2.28 123.2
OP3	Y38 OH		Y38 OH			Y38 OH
	1.74 148.3		1.76 160.2			1.76 150.4
	R77 NE		R77 NE			E58 OE2
	2.34 133.1		1.78 145.3			1.78 134.3
H	E58 OE1		E58 OE1	E58 OE1	E58 OE1	E58 OE1
	1.69 143.0		1.69 152.0	1.69 161.7	1.69 164.9	1.77 123.9

[a] The criteria followed for selecting hydrogen bonds are the same as suggested by Baker and Hubbard.[18]

[b] Distance between the hydrogen and the acceptor atoms (in Ångstroms) and the angle formed by the donor, hydrogen, and the acceptor atoms (in degrees) are also shown.

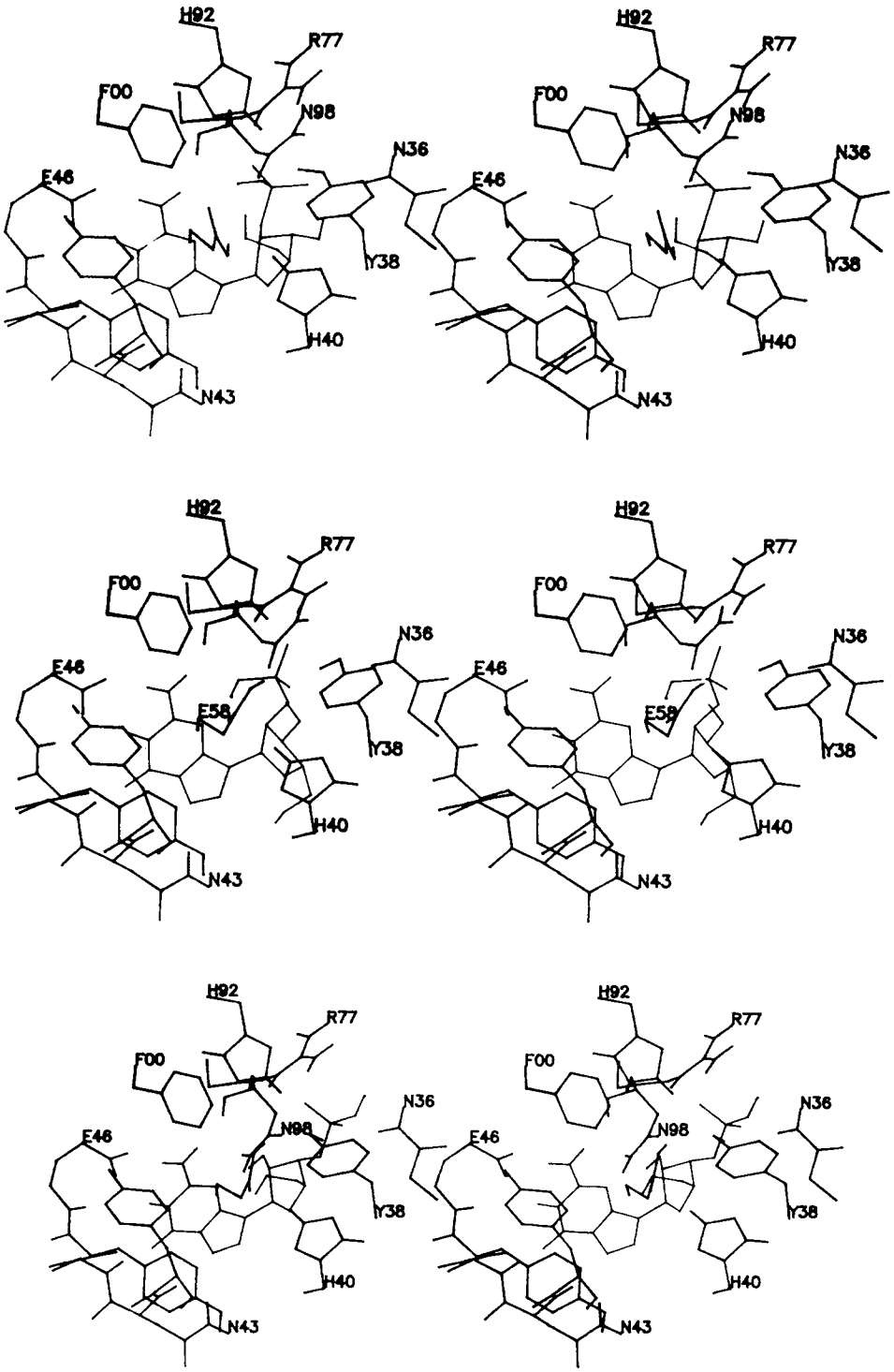

Figure 2 Stereo diagrams viewed down the *Z* axis of the complexes of the three inhibitors 2′-GMP, 3′-GMP, and 5′-GMP in both C2′-*endo* and C3′-*endo* conformations with RNase T_1 in their minimum energy conformations. Only those residues involved directly in binding are shown without the backbone N, H, C, and O atoms (except for Asn98) for clarity. The protein atoms are connected by thick lines and the inhibitor atoms by thin lines. The

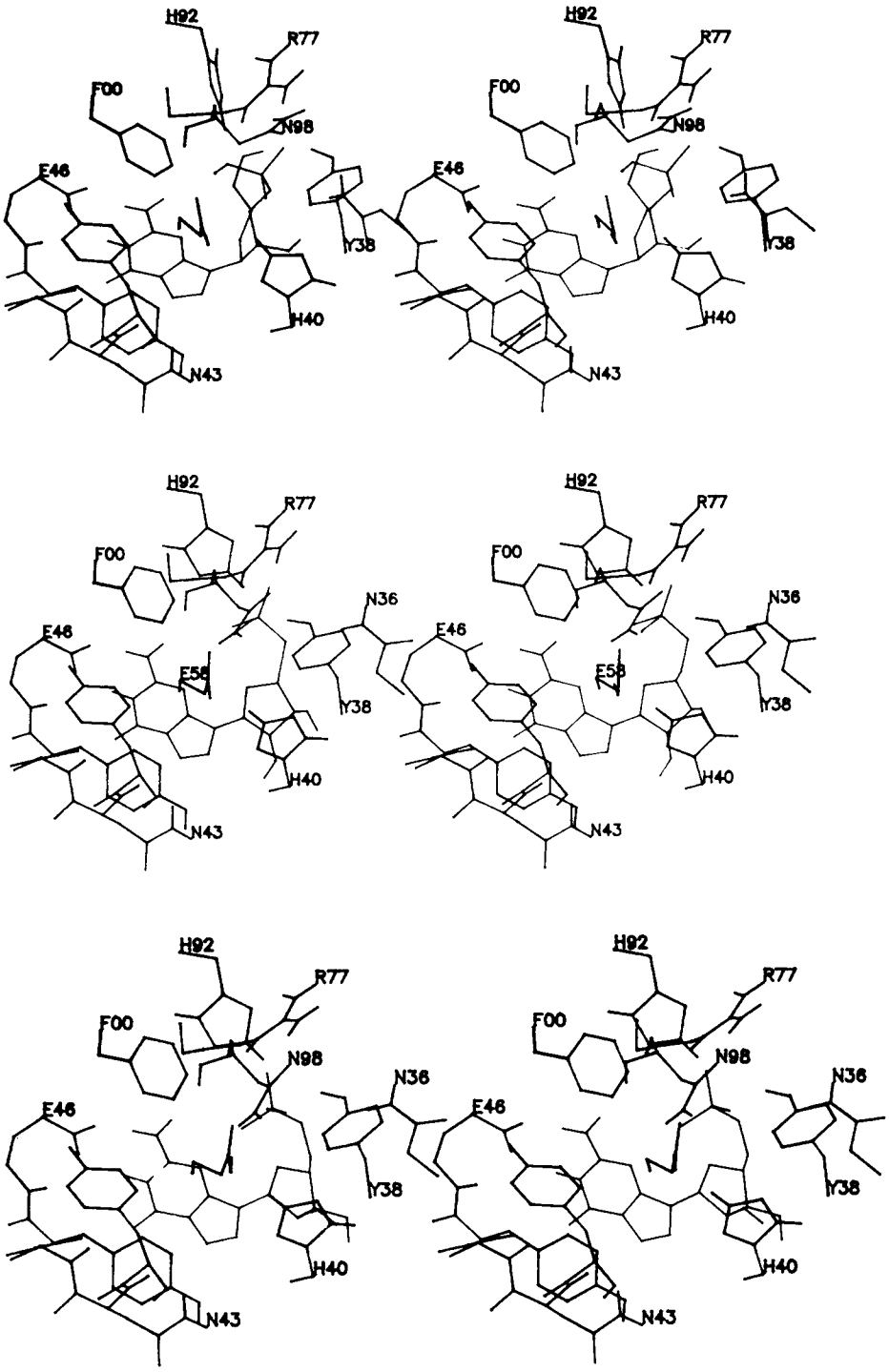

Figure 2. (*Continued from the previous page.*) single-letter amino acid codes used are N: Asn; H: His; Y: Tyr; R: Arg; E: Glu; F: Phe. F00 stands for phenyl alanine 100. (a) 2′-GMP (C2′-*endo*)–RNase T_1 complex. (b) 2′-GMP (C3′-*endo*)–RNase T_1 complex. (c) 3′-GMP (C2′-*endo*)–RNase T_1 complex. (d) 3′-GMP (C3′-*endo*)–RNase T_1 complex. (e) 5′-GMP (C2′-*endo*)–RNase T_1 complex. (f) 5′-GMP (C3′-*endo*)–RNase T_1 complex.

Table X Side-Chain Conformation of the Amino Acid Residues in the Minimum Energy Complexes of the Inhibitors with RNase T_1[a]

Residue[b] Name	Crystal[c] Structure	Calculated Torsion Angle Values					
		C2′-*endo*			C3′-*endo*		
		2′-GMP	3′-GMP	5′-GMP	2′-GMP	3′-GMP	5′-GMP
Ser35 CA-CB	−78	53	53	53	54	55	53
Asn36 CA-CB	−60	−51	−41	−48	−48	−139	−50
Asn36 CB-CG	−6	−167	172	−177	−178	166	−169
Ser37 CA-CB	−74	−60	−60	−60	−60	−60	−60
Tyr38 CA-CB	−69	−76	−90	−71	−70	−62	−78
His40 CA-CB	66	51	52	57	55	51	53
His40 CB-CG	62	−125	−119	−126	−128	−136	−125
Lys41 CB-CG	173	−157	−157	−157	−157	−157	−157
Lys41 CD-CE	162	−168	−168	−170	−169	−170	−169
Asn43 CA-CB	−62	−61	−56	−61	−60	−62	−58
Asn43 CB-CG	−78	108	97	99	102	100	99
Glu46 CG-CD	20	20	42	33	19	39	37
Asp49 CA-CB	−122	−162	−162	−162	−162	−162	−162
Asp49 CB-CG	−145	−63	−63	−63	−63	−63	−63
Tyr56 CB-CG	−57	−67	−67	−67	−67	−67	−67
Glu58 CA-CB	66	48	58	59	56	48	66
Glu58 CB-CG	174	174	157	170	152	178	147
Glu58 CG-CD	−96	163	−48	132	−66	153	140
Ser72 CA-CB	−168	179	179	179	179	179	179
Asp76 CB-CG	−27	−44	−44	−44	−44	−44	−44
Arg77 CA-CB	−49	−42	−38	−44	−37	−45	−41
Arg77 CB-CG	−72	−63	−63	−61	−63	−61	−61
Arg77 CG-CD	−176	172	175	172	−174	174	176
Arg77 CD-NE	−96	−134	−144	−130	−145	−131	−137
Arg77 NE-CZ	−5	13	14	8	15	14	14
Val78 CA-CB	152	176	176	176	176	176	176
His92 CA-CB	−72	−78	−78	−81	−76	−61	−81
His92 CB-CG	134	−16	−15	−9	−19	89	−9
Thr93 CA-CB	−63	−42	−42	−42	−42	−42	−42
Asn98 CA-CB	−98	−153	55	−156	−151	−88	−157
Asn98 CB-CG	−75	83	87	−95	74	80	−98
Phe00 CA-CB	−78	−82	−82	−81	−86	−56	−80
Phe00 CB-CG	−80	−70	−70	−72	−62	−100	−73

[a] Phe00 stands for phenyl alanine 100. Only those side-chain torsion angles that alter by more than 10° from the crystal structure conformation are listed here. The definition of the various torsion angles are as given in Ref. 19.
[b] Name of the amino acid residue and the bond about which significant change in torsion angle is noted.
[c] Torsion angle value reported in the 2′-GMP–Lys25–RNase T_1 complex.[11]

chains form a hydrogen bond with the phosphate in the 2′-GMP–RNase T_1 (both C2′-*endo* and C3′-*endo*) and 3′-GMP(C2′-*endo*)–RNase T_1 complexes, and two hydrogen bonds in the 5′-GMP–RNase T_1 (C2′-*endo*) complex. In the 5′-GMP(C3′-*endo*)–RNase T_1 complex, Arg77 forms one and His92 forms two hydrogen bonds with the phosphate group. In the 3′-GMP(C3′-*endo*)–RNase T_1 complex, Arg77 forms two hydrogen bonds with the phosphate group. The total conformational energy difference between the C2′-*endo* and C3′-*endo* pucker forms of the 2′-GMP–RNase T_1 and 3′-GMP–RNase T_1 complexes is negligibly small. However, the 5′-GMP(C3′-*endo*)–RNase T_1 complex has slightly higher conformational energy (1.5 kcal/mol) than the 5′-GMP(C2′-*endo*)–RNase T_1 complex. Thus the binding of 2′-GMP and 3′-GMP in both C2′- and C3′-*endo* ribose pucker forms to

RNase T_1 is equally probable, whereas for 5′-GMP, C2′-*endo* pucker form is slightly more favoured over C3′-*endo* form.

DISCUSSION

In the 2′-GMP(C2′-*endo*)–RNase T_1 complex, the number of hydrogen bonds between the base and the protein predicted here are slightly more than those reported from either of the two crystal structure studies[11,12] (Table I). The hydrogen bond between the side-chain amide group of Asn43 and N7 of guanine predicted from the present calculations is not reported by Arni et al.[11] In the native 2′-GMP–RNase T_1 complex, although this Asn43 ND2–N7 hydrogen bond has been reported, the Tyr45 N–O6 and Glu46 OE2–N2 hydrogen bonds are not reported.[12] Thus the present calculations indicate that all the hydrogen bonds proposed between the guanine base and the enzyme in the complex of 2′-GMP with both the native and Lys25–RNase T_1 are possible. The O2′ and O5′ atoms of ribose can form hydrogen bonds with His40 NE2, Glu58 OE2, and Asn98 OD1 of the protein. These hydrogen bonds are not indicated in any of the crystal structure studies. For the phosphate, there is a better agreement between the hydrogen bonds proposed from the present calculations and those reported in the native 2′-GMP–RNase T_1 complex.

A stereo diagram comparing the energy-minimized structure obtained from this study for the 2′-GMP(C2′-*endo*)–RNase T_1 complex with the structure obtained by the 1.9 Å resolution x-ray crystallographic study of 2′GMP–Lys25–RNase T_1 is shown in Figure 3. The rms differences in the positions of the amino acid side-chain atoms between the initial x-ray structure and the final energy-minimized structure are tabulated in Table XI. For the inhibitor 2′-GMP molecule, the rms difference is 2.09 Å. Side chains of residues Ser35, Asn36, His40, Lys41, Asn43, Asp49, Glu58, Arg77, Val78, His92, and Asn98 show considerable deviation from the starting conformation. The orientation of the base in the theoretically predicted complex is nearly the same as that observed in the x-ray crystallographic study, but the ribose–phosphate conformation is slightly different. Amino acid residues that are directly involved in binding and catalysis—viz., Asn36, His40, Asn43, Glu58, Arg77, His92, and Asn98—deviate from the initial conformation to have better hydrogen-bonding interactions with the bound inhibitor. The movement of the side chains of the amino acid residues in the active site appear to be concerted whereas those that are away from the active site move mainly to relieve unfavorable interactions present in the reported x-ray structure.

The present calculations also predict that the mode of binding of 3′-GMP and 5′-GMP is very similar to that of 2′-GMP as inferred from the ^{1}H-nmr studies.[13] The base and the phosphate moieties interact with the same amino acid residues in all three RNase T_1–inhibitor complexes, which requires the relative disposition of the base and the phosphate to be the same, independent of the phosphate position on the inhibitor. This is possible due to the flexibility of the inhibitor, which allows rotation of the base about the glycosyl bond and alterations in

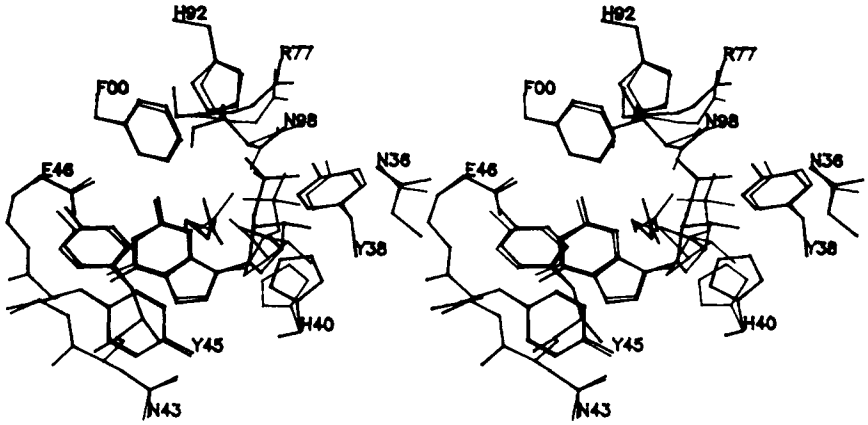

Figure 3 Stereoscopic projection of the 2′-GMP–Lys25–RNase T_1 complex obtained from the 1.9 Å resolution x-ray crystallographic study[11] (thick lines) superimposed over the 2′-GMP(C2′-*endo*)–RNase T_1 structure arrived at from the present calculations (thin lines).

Table XI Root Mean Square Differences (Å) in the Position of the Side-Chain Atoms of the Amino Acids in the 2′-GMP–RNase T_1 Complex Between the X-Ray and Energy-minimized Structures[a]

Amino Acid	Root Mean Square Difference	Amino Acid	Root Mean Square Difference
Ser 35	2.515	Ile 61	0.137
Asn 36	1.873	Tyr 68	0.093
Ser 37	0.342	Ser 69	0.056
Tyr 38	0.407	Ser 72	0.291
His 40	1.812	Asp 76	0.429
Lys 41	0.997	Arg 77	0.589
Tyr 42	0.248	Val 78	0.569
Asn 43	1.848	Val 79	0.202
Asn 44	0.331	Val 89	0.178
Tyr 45	0.159	Ile 90	0.137
Glu 46	0.283	Thr 91	0.009
Phe 48	0.121	His 92	1.612
Asp 49	1.676	Thr 93	0.528
Phe 50	0.078	Ser 96	0.226
Tyr 56	0.164	Asn 98	2.304
Tyr 57	0.013	Asn 99	0.382
Glu 58	1.382	Phe 100	0.243
Trp 59	0.043	Val 101	0.128

[a] Coordinates for the side-chain atoms of Glu102 were not available from the x-ray study.

the ribose pucker. A change in the ribose pucker affects a large change in the glycosyl angle of the bound inhibitor in the 2′-GMP–RNase T_1 and 3′-GMP–RNase T_1 complexes, but not in the 5′-GMP–RNase T_1 complex (Table VIII). In all the three RNase T_1–inhibitor complexes, the ribose moiety forms at least one hydrogen bond with the protein. This suggests that the ribose moiety does not act merely as a spacer between the base and the phosphate to ensure proper disposition between them for binding as indicated earlier,[13] but it also contributes significantly to the stability of the complex. The contribution of the ribose moiety towards the binding energy is more in the 2′-GMP–RNase T_1 and the 3′-GMP–RNase T_1 complexes in comparison to the 5′-GMP–RNase T_1 complex where the Asn98 ND2 to ribose O4′ hydrogen bond is rather weak. Although His92 was found to be present in the phosphate binding site in the complex of 2′-GMP with both the native- and Lys25–RNase T_1, no hydrogen bond was reported between His92 and the phosphate group from the x-ray diffraction studies. The present calculations show that His92 may indeed form one hydrogen bond with the phosphate group in the 2′-GMP–RNase T_1 (both C2′-*endo* and C3′-*endo*) and 3′-GMP(C2′-*endo*)–RNase T_1 complexes, and a bifurcated hydrogen bond with the two phosphate oxygen atoms in the 5′-GMP–RNase T_1 (both C2′-*endo* and C3′-*endo*) complexes. However, in the 3′-GMP(C3′-*endo*)–RNase T_1 complex, His92 may form a hydrogen bond with the phosphate group instead of O5′ of ribose. Such a switch in the hydrogen bond increases the total conformational energy by about 1 kcal/mol over the minimum energy conformation.

It can be seen from Table VIII that of the three RNase T_1–inhibitor complexes, the 2′-GMP–RNase T_1 complex has the least and the 5′-GMP–RNase T_1 complex has the highest total conformational energy, suggesting that the former forms a more stable complex than the latter. This is qualitatively in agreement with gel filtration, uv-difference spectral, and kinetic studies[8,35-39] showing that the binding affinity and the inhibitory effect of the three nucleotide inhibitors decreases in the order 2′-GMP > 3′-GMP > 5′-GMP (Table XII). In the 2′-GMP–RNase T_1 complex, Glu58 forms hydrogen bond with the phosphate (Figure 2a,b and Table IX). This may explain the unusually high pK_a of Glu58 reported from the potentiometric and spectrophotometric titration studies.[3] Such an interaction between the phosphate and Glu58 is possible in other complexes also except in the 3′-GMP(C2′-*endo*)–RNase T_1 complex.

In the complexes of the three mononucleotide inhibitors 2′-GMP, 3′-GMP, and 5′-GMP with RNase T_1 (Table VIII), the ribose pucker, be it C2′-*endo* or C3′-*endo*, makes very little difference to the total conformational energy of the complex, indicating that in solution both may be present and in solid state it may be frozen in either form. The present calculations predict that the glycosyl torsion angle in the 2′-GMP(C2′-*endo*)–RNase T_1 complex will be in the +sc range (85°), which is in fairly good agreement with the x-ray crystal structure studies (55° in the 2′-GMP–Lys25–RNase T_1 complex). The same torsion angle in the 2′-GMP(C3′-*endo*)–

Table XII Standard Free Energy of Binding of the RNase T_1–GMP Complexes ($-\Delta G^\circ$ in kcal/mol)

	Ref. 8	Ref. 35	Ref. 36	Ref. 37	Ref. 38
2′-GMP	5.6	7.04	6.3	7.1	6.9
3′-GMP	5.18	6.44	4.7	7.	6.7
5′-GMP	3.97	5.37	2.7	5.7	6.2

RNase T_1 complex falls in the +anticlinal (+ac) range (137°). In the case of the 3′-GMP(C3′-*endo*)–RNase T_1 and the 3′-GMP(C2′-*endo*)–RNase T_1 complexes, this angle favors values of 7° and 88°, respectively, in the +synperiplanar (+sp) and +sc ranges. These are in agreement with those assumed in the interpretation of the nmr data.[13] On the other hand, in the 5′-GMP–RNase T_1 complex, the glycosyl torsion angle favors a value in the −synclinal (−sc) range (−53° if the ribose is in C2′-*endo* puckered form and −73° if the ribose is in C3′-*endo* puckered form), which is in disagreement with the orientation assumed (*anti*) by Inagaki et al.[13] to interpret the nmr data. The distances between the hydrogen atoms attached to C8 of guanine (H8) and C1′ of ribose (H1′) in the minimum energy conformation of the three inhibitor–protein complexes are also shown in Table VIII. This H8–H1′ distance is about 2.6 Å in the 2′-GMP(C2′-*endo*)–RNase T_1 complex and 3.9 Å in the 2′-GMP(C3′-*endo*)–RNase T_1 complex. Therefore a large nuclear Overhauser enhancement (NOE) is to be expected for the H1′ proton resonance on irradiation of the H8 proton only if the bound 2′-GMP molecule in the complex with RNase T_1 adopts C2′-*endo* and not the C3′-*endo* ribose puckering mode. The large NOE reported for the pair of H1′ and H8 protons of guanosine clearly suggests that the ribose moiety of the bound 2′-GMP molecule adopts the C2′-*endo* puckered conformation in significant amounts. The vicinal coupling constant of about 4.5 Hz observed in the 1 : 1 mole ratio complex is intermediate between the values of 2 and 8 Hz expected for C3′-*endo* and C2′-*endo* puckered conformations, respectively. This indicates that the ribose moiety in the 2′-GMP–RNase T_1 complex should exist in both the puckered conformations. Thus the nmr results on the 2′-GMP–RNase T_1 complex are consistent with the theoretical predictions, i.e., in solution the ribose moiety may occur in both the puckered conformations as the difference in the total conformational energy between the 2′-GMP(C2′-*endo*)–RNase T_1 and the 2′-GMP(C3′-*endo*)–RNase T_1 complexes is negligibly small (Table VIII). It should be recalled that while interpreting the nmr data, Inagaki et al.[13] considered only the C3′-*endo* pucker conformation. In the 3′-GMP–RNase T_1 complex a large NOE should be expected in both the C2′-*endo* (H1′-H8 distance = 2.6 Å) and the C3′-*endo* (H1′-H8 distance = 2.8 Å) ribose pucker conformations. Hence NOE studies may not throw any light on the nature of the ribose pucker in this case. The observed vicinal coupling constant of 4–6 Hz in the 1 : 1 mole ratio complex of 3′-GMP with RNase T_1 suggests the possibility of existence of both the puckered conformations of ribose in solution. This is again consistent with the theoretical predictions that in solution the ribose moiety in the 3′-GMP–RNase T_1 complex may occur in both puckered conformations as the energy difference between the 3′-GMP(C2′-*endo*)–RNase T_1 and the 3′-GMP(C3′-*endo*)–RNase T_1 complexes also is very small. In the 5′-GMP–RNase T_1 complex the distance between the H1′-H8 protons is about 3.5 Å in either of the puckered conformations and hence the expected NOE is negligibly small, which in fact is the case. The energy difference between the 5′-GMP(C2′-*endo*)–RNase T_1 and the 5′-GMP(C3′-*endo*)–RNase T_1 complexes is small (1.5 kcal/mol), with the C2′-*endo* conformation being slightly favored over C3′-*endo* conformation; but the observed vicinal coupling constants suggest that the 5′-GMP binds predominantly in the C3′-*endo* puckered conformation. It is also important to note that theoretical calculations on the guanosine 3′,5′-bis(phosphate)–RNase T_1 complex (unpublished results) predict that the 5′-phosphate end binds in the phosphate binding site in preference to the 3′-phosphate end with the ribose moiety in C3′-*endo* puckered conformation, in agreement with the nmr studies.

Chemical modification and spectroscopic studies have shown that His40, Glu58, Arg77, and His92 are actively involved in the catalysis of RNase T_1. Although there is consensus that His92 serves to protonate the O5′ oxygen of the leaving group, the attack at the 2′ hydroxyl is still a matter of debate. Does Glu58 act as a base (which appears probable due to its high pK_a value in the presence of bound nucleotide) with His40 engaged in its activation,[40] or is it His40 that accepts the proton? The present work cannot provide an answer, although in the complex of 3′-GMP (which resembles the substrate more closely than 2′-GMP and 5′-GMP) with RNase T_1, the 2′-hydroxyl group is in hydrogen bonding contact only to Glu58 and only if the ribose pucker is C2′-*endo*. More theoretical and experimental studies are necessary to clarify this point.

CONCLUSIONS

The theoretical models arrived at from the present study suggest that in the complexes of 2′-GMP, 3′-GMP, and 5′-GMP with RNase T_1, the ribose moiety may be present in both the puckered conformations to significant extents in solution whereas in the solid state it may be frozen in either of the two conformations. These studies also explain the

relative inhibitory effect of these three inhibitors and the high pK_a value observed for Glu58 in the presence of 2′-GMP. These predicted models are also consistent in general with the ^{1}H-nmr data. It is interesting to note that in a recently reported x-ray crystal structure study of guanylyl-2′,5′-guanosine–RNase T_1,[41] the ribose of the guanosine 2′-phosphate moiety adopts two conformations—C2′-*endo* and C3′-*endo*—in a statistical ratio 30 : 70 and this corroborates well with the predictions of the present study that the ribose can occur in either of the two puckered forms.

REFERENCES

1. Irie, M. (1964) *J. Biochem.* (Tokyo) **56,** 495–497.
2. Irie, M. (1967) *J. Biochem.* (Tokyo) **61,** 550–554.
3. Iida, S. & Ooi, T. (1969) *Biochemistry* **8,** 3897–3902.
4. Walz, F. G. Jr. (1977) *Biochemistry* **16,** 4568–4571.
5. Arata, Y., Kimura, S., Matsuo, H. & Narita, K. (1979) *Biochemistry* **18,** 18–24.
6. Inagaki, F., Kawano, Y., Shimada, I., Takahashi, K. & Miyazawa, T. (1981) *J. Biochem.* (Tokyo) **89,** 1185–1195.
7. Sato, S. & Egami, F. (1965) *Biochem. Z.* **342,** 437–448.
8. Epinatjeff, C. & Pongs, O. (1972) *Eur. J. Biochem.* **26,** 434–441.
9. Egami, F., Oshima, T. & Uchida, T. (1980) *Mol. Biol. Biochem. Biophys.* **32,** 250–277.
10. Takahashi, K. & Moore, S. (1980) *Enzymes* **15,** 435–468.
11. Arni, R., Heinemann, U., Tokuoka, R. & Saenger, W. (1988) *J. Biol. Chem.* **263,** 15358–15368.
12. Sugio, S., Amisaki, T., Ohishi, H. & Tomita, K. (1988) *J. Biochem.* (Tokyo) **103,** 354–366.
13. Inagaki, F., Shimada, I. & Miyazawa, T. (1985) *Biochemistry* **24,** 1013–1020.
14. Sugio, S., Oka, K., Ohishi, H., Tomita, K. & Saenger, W. (1985) *FEBS Lett.* **183,** 115–118.
15. Taylor, R. & Kennard, O. (1982) *J. Mol. Struct.* **78,** 1–28.
16. Saenger, W. (1984) *Principles of Nucleic Acid Structure,* Springer-Verlag, New York.
17. Arnott, S. & Hukins, D. W. L. (1972) *Biochem. J.* **130,** 453–465.
18. Baker, E. N. & Hubbard, R. F. (1984) *Prog. Biophys. Mol. Biol.* **44,** 97–179.
19. Ramachandran, G. N. & Sasisekharan, V. (1968) *Adv. Protein Chem.* **23,** 283–437.
20. Momany, F. A., McGuire, R. F., Burgess, A. W. & Scheraga, H. A. (1975) *J. Phys. Chem.* **79,** 2361–2381.
21. Nemethy, G., Pottle, M. S. & Scheraga, H. A. (1983) *J. Phys. Chem.* **87,** 1883–1887.
22. Dunfield, L. G., Burgess, A. W. & Scheraga, H. A. (1978) *J. Phys. Chem.* **82,** 2609.
23. Thornton, J. M. & Bayley, P. M. (1975) *Biochem. J.* **149,** 585–596.
24. Bondi, A. (1964) *J. Phys. Chem.* **64,** 441–451.
25. Olson, W. K. & Flory, P. J. (1972) *Biopolymers* **11,** 25–56.
26. Yathindra, N. & Sundaralingam, M. (1973) *Biopolymers* **12,** 297–314.
27. Pople, J. A. & Beveridge, D. L. (1970) *Approximate Molecular Orbital Theory,* McGraw-Hill, New York.
28. Dennis, J. E., Jr. & Mei, H. H. W. (1979) *J. Opt. Theory Appn* **28,** 453–482.
29. Noguti, T. & Go, N. (1983) *J. Phys. Soc. Jpn.* **52,** 3685–3690.
30. Lakshminarasimhalu, P., to be published.
31. Gay, D. M. (1983) *ACM Trans. Math. Software* **9,** 502–524.
32. Chou, K. C., Nemethy, G., Rumsey, S., Tuttle, R. W. & Scheraga, H. A. (1986) *J. Mol. Biol.* **188,** 641–649.
33. Li, Z. & Scheraga, H. A. (1987) *Proc. Natl. Acad. Sci. USA* **84,** 6611–6615.
34. Gibson, K. D. & Scheraga, H. A. (1986) *Proc. Natl. Acad. Sci. USA* **83,** 5649–5653.
35. Walz, F. G., Jr. & Hooverman, L. L. (1973) *Biochemistry* **12,** 4846–4851.
36. Campbell, M. K. & Ts'o, P. O. P. (1971) *Biochim. Biophys. Acta* **232,** 427–435.
37. Takahashi, K. (1972) *J. Biochem.* (Tokyo) **72,** 1469–1481.
38. Oshima, T. & Imahori, K. (1971) *J. Biochem.* (Tokyo) **69,** 987–990.
39. Oshima, T. & Imahori, K. (1972) in Proteins Structure and Function, Vol. 1. (Ed. Funatsu, M., Hiromi, K., Imahori, K., Murachi, T. & Narita, K.) pp. 333–367.
40. Heinemann, U. & Saenger, W. (1982) *Nature* (London) **299,** 27–31.
41. Koepke, J., Maslowska, M., Heinemann, U. & Saenger, W. (1989) *J. Mol. Biol.* **206,** 475–488.

Received April 19, 1989
Accepted November 30, 1989